Appendix Figures

NELF-E is recruited to DNA double-strand break sites to promote transcription repression and repair

Samah W. Awwad, Enas R. Abu-Zhayia, Noga Guttmann-Raviv and Nabieh Ayoub[1]

Department of Biology, Technion - Israel Institute of Technology, Haifa 3200003, Israel.

This appendix file includes:

1. **Appendix Figure S1.** NELF-E knockdown leads to a degradation of NELF-B and NELF-A proteins.
2. **Appendix Figure S2.** ATM mediates transcription repression at DSB sites.
3. **Appendix Figure S3.** NELF-B and NELF-C/D show no accumulation at laser-microirradiated sites.
4. **Appendix Figure S4.** The N-terminal region, containing the LZ motif, is essential for NELF-E recruitment to laser microirradiated sites.
5. **Appendix Figure S5.** Expression of recombinant Flag-tagged NELF-E mutants.
6. **Appendix Figure S6.** Validating the suitability of NELF-E antibody for immunofluorescence analysis.
7. **Appendix Figure S7.** TNFα activates the expression of A20 gene.
8. **Appendix Figure S8.** TNFα treatment has no detectable effect on NELF-E protein levels.
9. **Appendix Figure S9.** ATM-independent recruitment of EGFP-NELF-E to laser-microirradiated sites.
10. **Appendix Figure S10.** Laser-microirradiation in control and PARP1 deficient U2OS cells.
11. **Appendix Figure S11.** NELF-E-E-Q mutant shows reduced level of ADP-ribosylation.
12. **Appendix Figure S12.** Evaluating the effect of α-amanitin treatment on the induction of DNA damage markers.

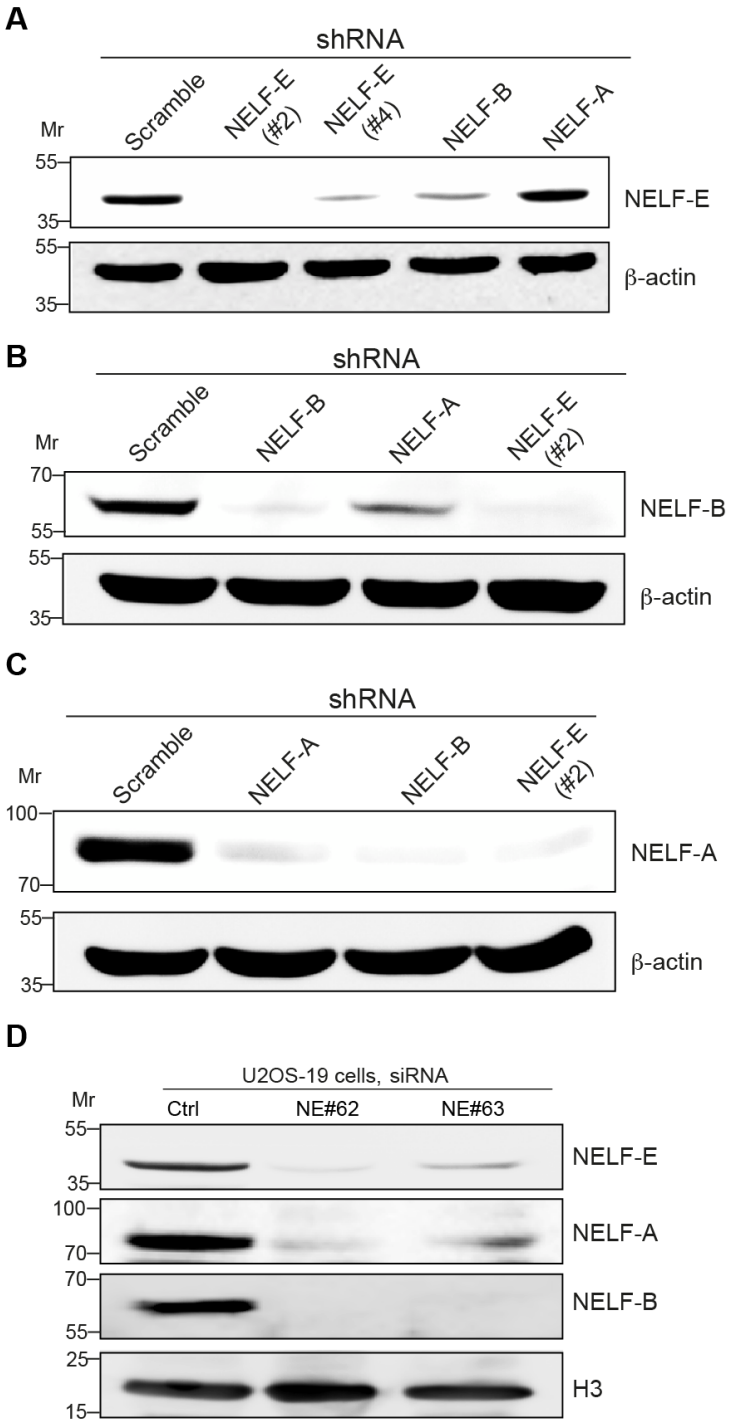

Appendix Figure S1. NELF-E knockdown leads to a degradation of NELF-B and NELF-A proteins. Western blots show the proteins levels of NELF-E (**A**), NELF-B (**B**) and NELF-A (**C**) in MCF7 cells expressing scramble shRNA or specific shRNA for NELF-A, NELF-B and NELF-E genes. β-actin was used as a loading control. In S1a, two shRNA sequences (#2; #4) for NELF-E were used. **(D)** Western blot shows the protein levels of NELF-E, NELF-A and NELF-B in U2OS-TRE-I-Sce-19 cells transfected with Ctrl or two different NELF-E siRNAs (#63 and #64). H3 was used as a loading control.

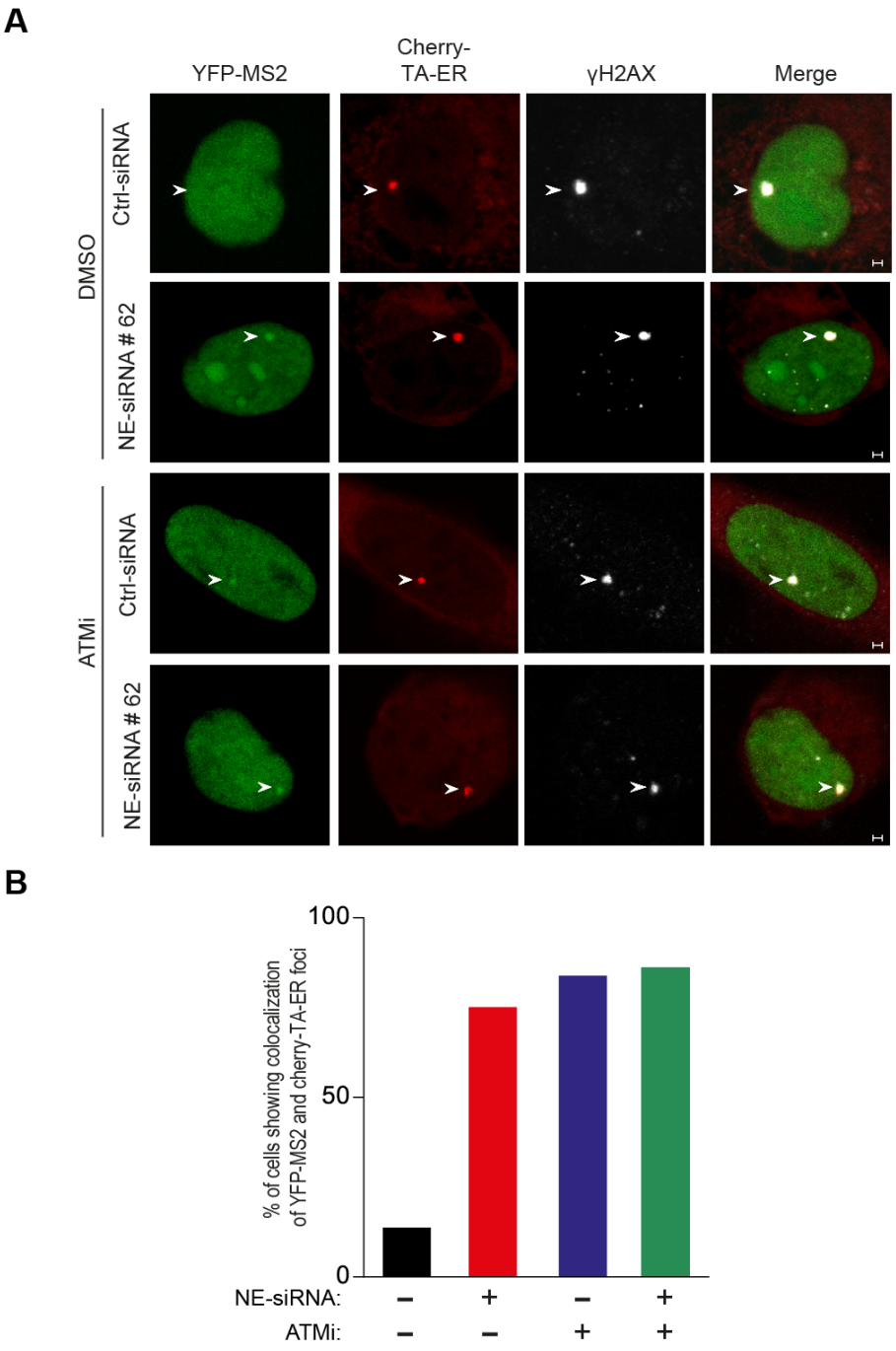

Appendix Figure S2. ATM mediates transcription repression at DSB sites.

(A) Mock and NELF-E-depleted U2OS-TRE-I-Sce-19 cells were transfected with pCherry-tTA-ER and pYFP-MS2 plasmids and treated with 10μM ATM inhibitor for 24hr, then cells were treated with 1μM tamoxifen for 2hr to activate transcription of MS2 gene. To induce DSB upstream the MS2 gene, cells were transfected with a third plasmid expressing I-Sce-I endonuclease. Cells were fixed and immunostained with γH2AX. Representative images were acquired using inverted confocal microscope. **(B)** Graph displays the percentage of cells that shows colocalization of YFP-MS2 and Cherry-tTA-ER. Data represent the mean of two independent experiments. The transcription of MS2 gene is marked with white arrowhead. Scale bar, 2μm.

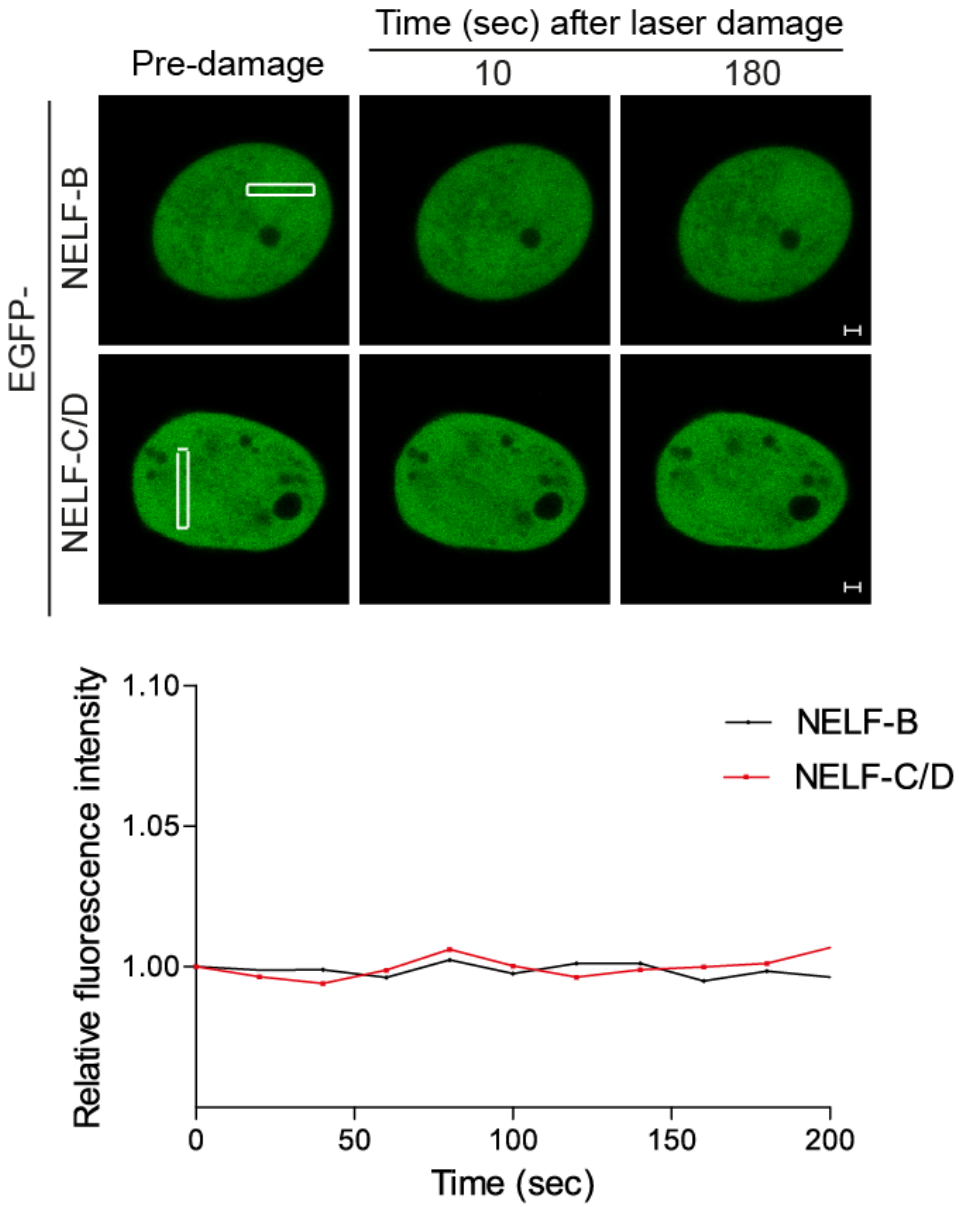

Appendix Figure S3. NELF-B and NELF-C/D show no accumulation at laser-microirradiated sites.

Representative time-lapse images showing the localization of EGFP-NELF-B and EGFP-NELF-C/D after laser-microirradiation targeted to a particular region marked by white rectangle. Graph in the bottom shows fold increase in the relative fluorescence intensity of NELF-B and NELF-C/D at laser-microirradiated sites. To achieve nuclear localization of EGFP-NELF-C/D or EGFP-NELF-B, U2OS cells were co-transfected with vector encoding Flag-NELF-A or Flag-NELF-E at a ratio of (1:1), respectively[1]. Results shown are typical of two independent experiments and represent 20 different cells. Scale bar, 2μm.

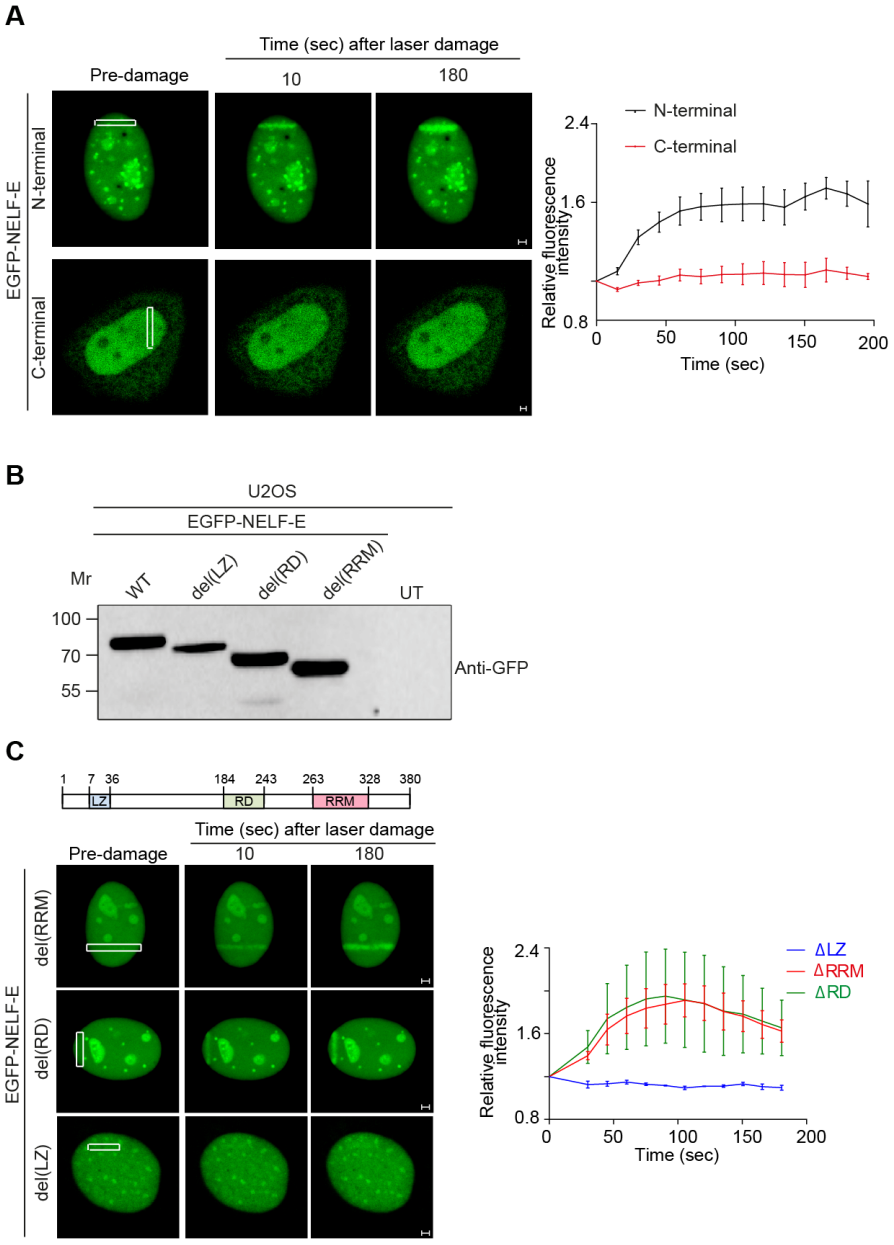

Appendix Figure S4. The N-terminal region, containing the LZ motif, is essential for NELF-E recruitment to laser microirradiated sites.

(A) Representative time-lapse images showing the localization of the N-terminal and the C-terminal of NELF-E at laser-microirradiated regions. U2OS cells were transfected with expression vectors encoding EGFP fused to the indicated deletion mutants of NELF-E and subjected to laser-microirradiation as in Fig. 2a. Graph shows fold increase in relative fluorescence intensity of the mutants at laser-microirradiated sites. Error bars represent SEM of 10 different cells (n=3). **(B)** Western blots show the proteins levels of EGFP-NELF-E wt, del (LZ), del (RD) and del (RRM) in U2OS cells. **(C)** as in (a), deletion mapping shows that the LZ motif, but not the RD or the RRM domains, of NELF-E is essential for its accumulation at laser-microirradiated sites (n=3). Schematic diagram of NELF-E depicting the position of the LZ, RD and the RRM domains is shown on top. Scale bar, 2μm.

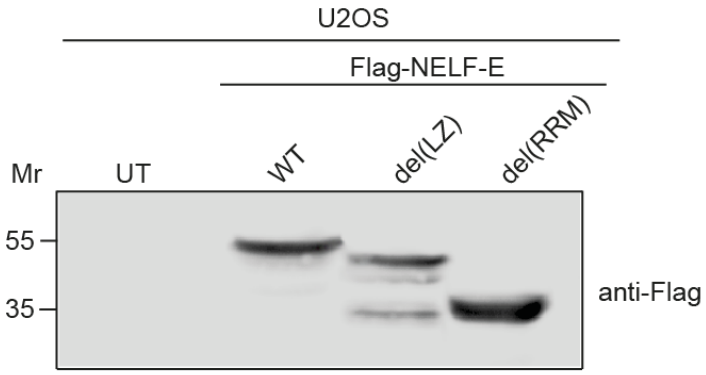

Appendix Figure S5. Expression of recombinant Flag-tagged NELF-E mutants. Western blot shows the expression of Flag-NELF-E, wild-type, del (LZ) and del(RRM) mutant in U2OS cells.

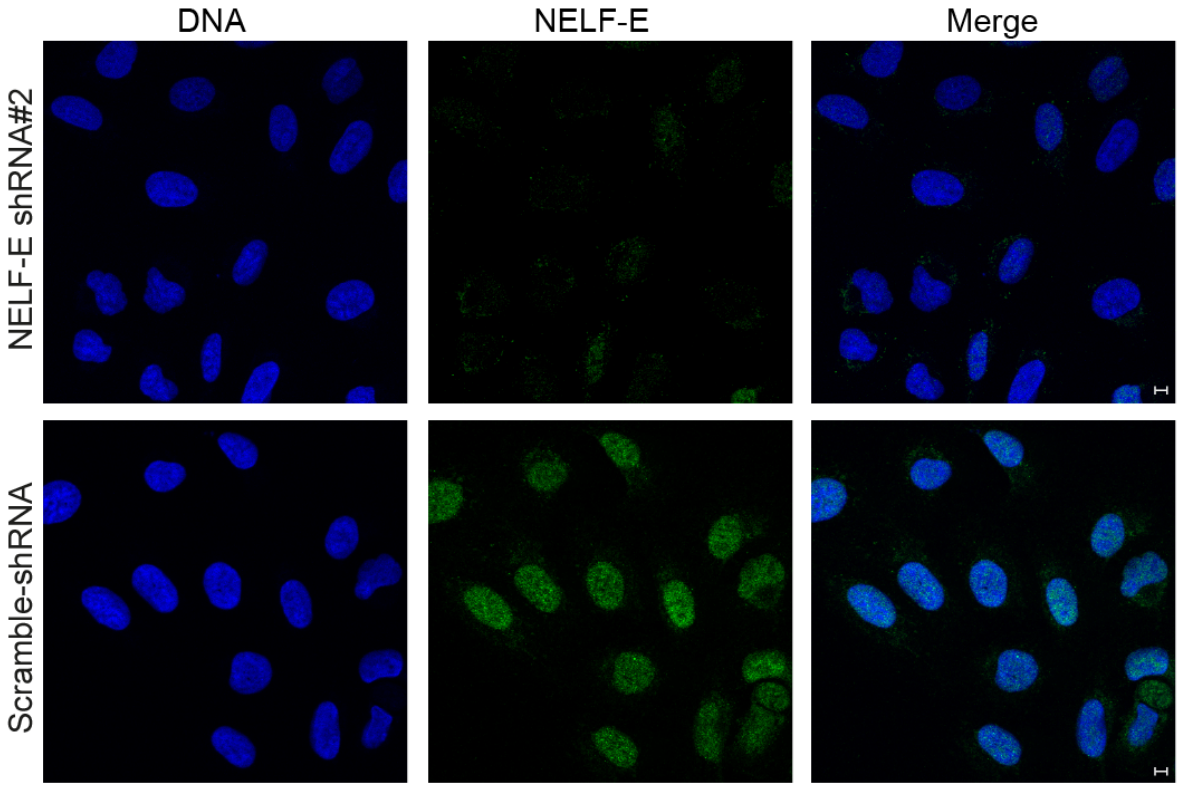

Appendix Figure S6. Validating the suitability of NELF-E antibody for immunofluorescence analysis. Representative field of cells showing that NELF-E antibody (Ab170104) recognizes the native form of NELF-E by immunofluorescence analysis. MCF7 cells expressing scramble shRNA or NELF-E shRNA#2 were fixed and immunostained using NELF-E antibody (green). DNA is stained with DAPI (blue). Results show dramatic decrease in the intensity of the green signal in MCF7 cells expressing NELF-E shRNA compared to cells expressing scramble shRNA. Scale bar, 10μm.

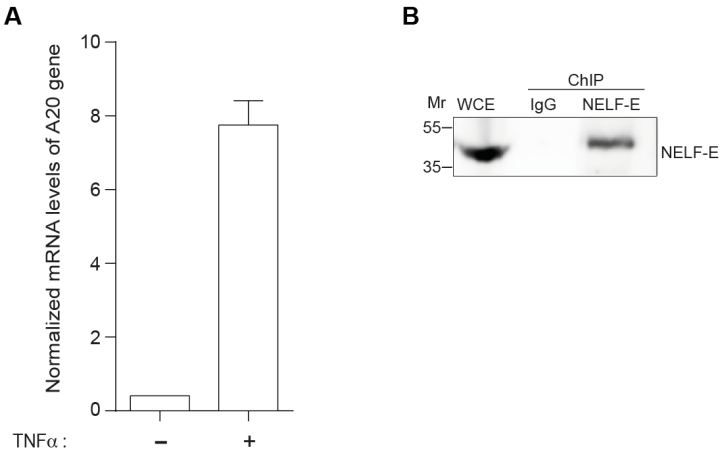

Appendix Figure S7. TNFα activates the expression of A20 gene.

(A) TNFα was added to the growth medium of Hela cells to a final concentration of 10ng/ml for 30min. Total RNA was then extracted using TRizol reagent and followed by first strand cDNA synthesis. SYBR green-based real-time quantitative PCR was performed to measure the transcript levels of A20 gene. The y-axis represents the relative mRNA level of A20, which was normalized to GAPDH transcripts. Results show ~8-fold increase in A20 expression following TNFα treatment. Error bars indicate SD (n=4). **(B)** Validating the suitability of NELF-E antibody for ChIP analysis. NELF-E ChIP was performed in Hela cells as described in materials and methods and immunoblotted with NELF-E antibody.

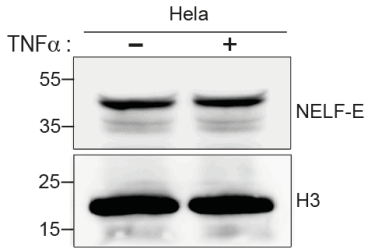

Appendix Figure S8. TNFα treatment has no detectable effect on NELF-E protein levels.

TNFα (10ng/ml) was added for 30 minutes to the growth medium of Hela cells to activate the expression of A20 gene. Cells were then lysed and subjected to western blot analysis using NELF-E antibody and H3 as a loading control.

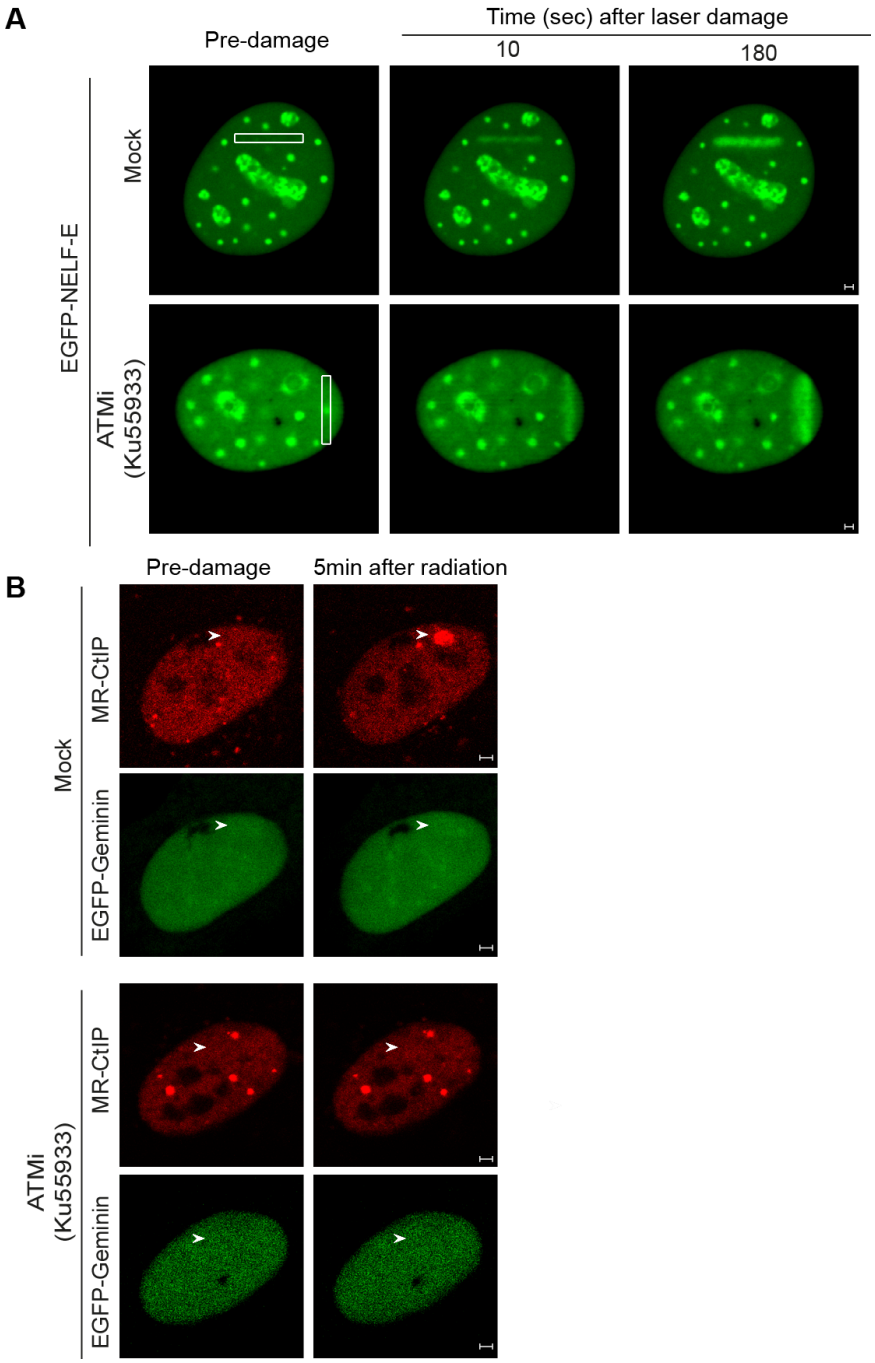

Appendix Figure S9. ATM-independent recruitment of EGFP-NELF-E to laser-microirradiated sites. (A) U2OS cells expressing EGFP-NELF-E fusion were treated for 2hr with 10μM ATM inhibitor (Ku-55933) prior to laser-microirradiation. Time-lapse images show the localization of EGFP-NELF-E fusion at the indicated time points after laser-microirradiation induction to a single region, marked by a white rectangle. **(B)** Representative time-lapse images showing the localization of MR-CtIP (red) at laser-microirradiated regions of U2OS cells that were untreated or treated with 10μM ATM inhibitor for 2hr. U2OS cells were co-transfected with expression vectors encoding MR-CtIP (Red) and EGFP fused to the N-terminal domain of Geminin (green) to mark cells at S/G2 stages. 15 green cells were subjected to laser microirradiation (n=2). Scale bar, 2μm.

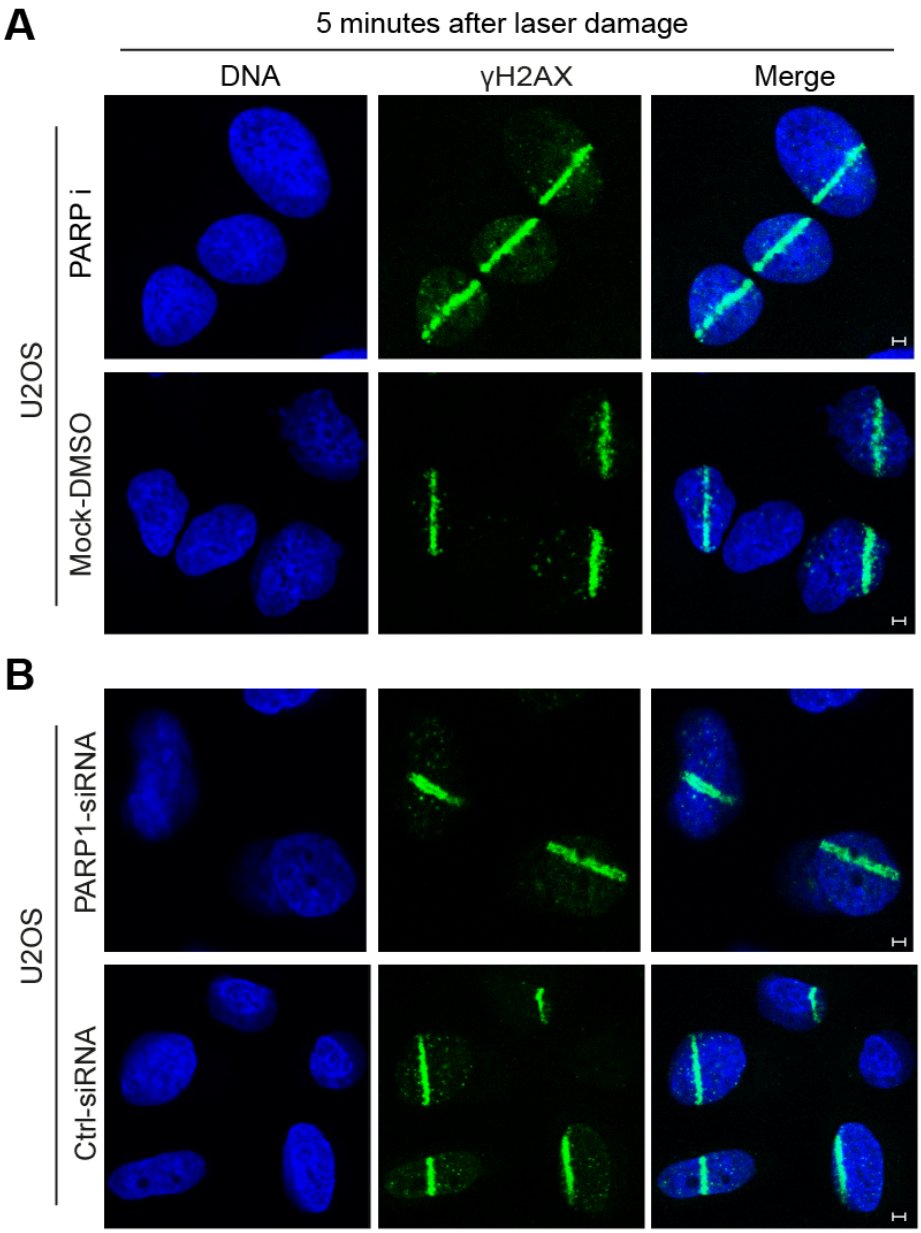

Appendix Figure S10. Laser-microirradiation in control and PARP1 deficient U2OS cells. Representative U2OS cells treated with PARP inhibitor **(A)** or depleted of PARP1 **(B)** were subjected to laser-microirradiation followed by immunofluorescence using γH2AX antibody (green). DNA is stained with DAPI (blue). Results shown are representative of at least 20 different cells of one biological repeat. Scale bar, 5μm.

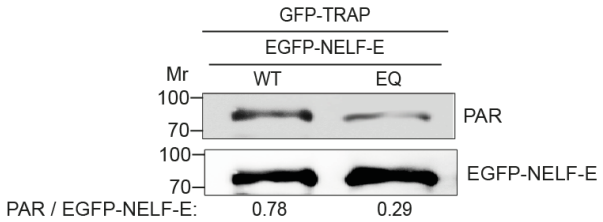

Appendix Figure S11. NELF-E-EQ mutant shows reduced level of ADP-ribosylation.
U2OS cells expressing either EGFP-NELF-E or EGFP-NELF-E-EQ mutant were subjected to GFP-TRAP and immunoblotted using PAR antibody.

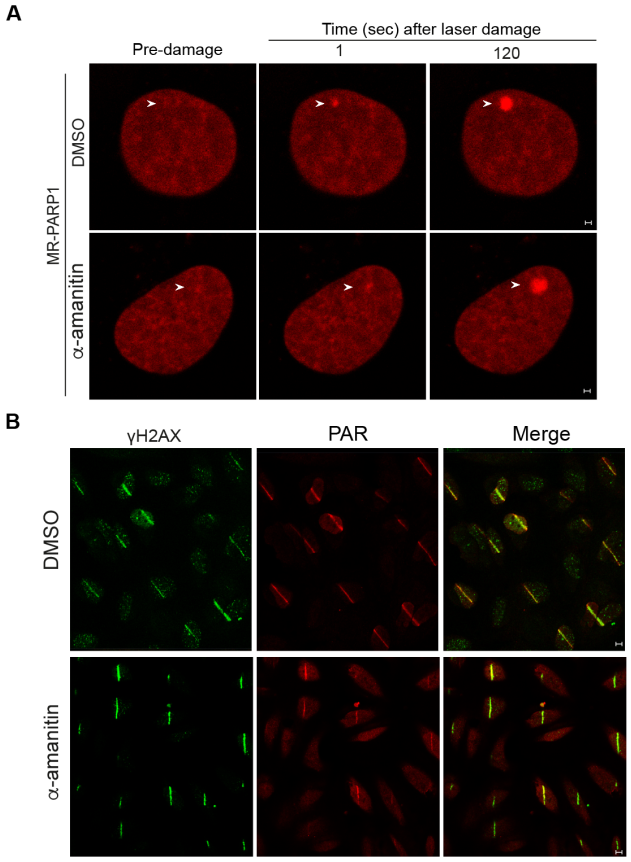

Appendix Figure S12. Evaluating the effect of α-amanitin treatment on the induction of DNA damage markers.
(A) PARP1 accumulation at laser-microirradiated sites is not affected by α-amanitin treatment. Representative time-lapse images showing the localization of MR-PARP1 at laser-microirradiated regions of cells that were untreated or treated with α-amanitin. Results shown are typical of 2 independent experiments. Scale bar, 2μm.
(B) U2OS cells were treated with α-amanitin or DMSO and subjected to laser microirradiation followed by immunofluorescence using γH2AX and PAR antibodies. Scale bar, 10μm.

Appendix References:

1. Yung TM, Narita T, Komori T, Yamaguchi Y, Handa H. Cellular dynamics of the negative transcription elongation factor NELF. *Exp Cell Res* **315**, 1693-1705 (2009).